https://doi.org/10.5194/egusphere-2026-2841
Preprint. Discussion started: 4 June 2026

The role of the QBO for tropical high-cloud variability in CMIP6 models and observations

Aleena M. Jaison[1], Paulo Ceppi[1], Sarah Wilson Kemsley[2]

[1]Department of Physics, Imperial College London, London, United Kingdom
[2]School of Geography and the Environment, University of Oxford, Oxford, United Kingdom

Correspondence to: Aleena M. Jaison (a.moolakkunnel-jaison@imperial.ac.uk)

Abstract. The Quasi-Biennial Oscillation (QBO) is a dominant mode of stratospheric zonal wind variability. Observations indicate that the QBO influences tropical phenomena such as convection, precipitation, and the Madden–Julian Oscillation, yet climate models often fail to capture these relationships. This study examines the QBO's impact on high clouds, in particular tropical tropopause layer clouds, in CMIP6 historical simulations and CALIPSO observations. Building on recent findings that identified relevant cloud-controlling factors (CCFs) for high clouds, we apply CCF analysis to assess QBO-driven changes in high-cloud amount and interpret these changes in terms of contributions from controlling factors. Our results confirm that the QBO westerly (QBOW) phase is associated with reduced tropical mean high-cloud cover. CMIP6 models successfully capture the reduction in tropical high clouds associated with QBOW, but with a weaker magnitude and strong inter-model spread. Among the analysed CCFs, upper-tropospheric temperature, static stability at 150hPa and relative humidity contribute most to this reduction in observations, and to the model bias. The substantial model bias and spread suggest that better constraints on high-cloud sensitivity to upper-tropospheric thermodynamics are needed to improve simulated QBO-related cloud responses. This framework may also help assess cloud responses to climate change, including the role of greenhouse gas–driven stratospheric cooling.

1 Introduction

The quasi-biennial oscillation (QBO) is a prominent mode of stratospheric variability that plays a significant role in the stratosphere-troposphere interactions. The QBO is characterised by alternating westerly and easterly zonal winds in the tropical stratosphere, extending from 10hPa to 70hPa with a mean periodicity of approximately 28 months (Holton and Lindzen, 1972; Lindzen and Holton, 1968; Plumb and Bell, 1982). Beyond its stratospheric features, the QBO exerts a range of influences on the troposphere, from impacting tropical convection and the Madden–Julian Oscillation (MJO) to affecting extratropical weather patterns, for example via the polar vortex (Baldwin et al., 2001; Collimore et al., 2003; Gray et al., 2018; Yoo and Son, 2016). While robust observational evidence exists on the QBO's downward influence on tropical convection, cloud variability, and the MJO, climate models often struggle to accurately capture these effects (Kim et al., 2020; Lim and Son, 2020).

https://doi.org/10.5194/egusphere-2026-2841
Preprint. Discussion started: 4 June 2026

The QBO–cloud relationship has been increasingly gaining attention in recent years (Davis et al., 2013; Sweeney et al., 2023; Sweeney and Fu, 2024; Tseng and Fu, 2017). Clouds are a key component of our climate system, playing a significant role in Earth's energy budget. Under greenhouse gas forcing, cloud feedback remains one of the largest uncertainties in climate projections. A major accepted cloud feedback mechanism is through the increase in upper-level cloud altitude with warming (Ceppi et al., 2017). Changes in amount and thickness of tropical anvil clouds are also highlighted in literature (Wilson Kemsley et al., 2025). The internal variability of these clouds has been linked to QBO, along with other modes of variability such as ENSO and the Brewer–Dobson circulation (BDC). Given recent suggestions that the QBO may weaken or disappear under global warming (Luo et al., 2026), understanding the QBO–cloud relationship is increasingly important. The QBO could also serve as a proxy to understand how clouds respond to global warming. As QBO-related temperature variations are well-observed, QBO–cloud relationships may help us to infer how stratospheric cooling associated with global warming could be affecting clouds.

Observations indicate that the QBO westerly phase, defined by westerly zonal winds in the tropical lower stratosphere, is associated with reduced tropical cloudiness and convection (Collimore et al., 2003; Gray et al., 2018; Sweeney et al., 2023). While ENSO contributes substantially to zonally resolved variability in tropical tropopause layer (TTL) clouds, the QBO has been identified as the dominant driver of zonal-mean high-cloud variability in the deep tropics (Davis et al., 2013; Tseng and Fu, 2017). Both ENSO and QBO are noted to be leading factors in TTL cirrus cloud spatial and temporal distribution (Tseng and Fu, 2017). The QBO also exerts strong control on cold-point temperature, water vapor, and cloud fraction, particularly during May-September (Sweeney and Fu, 2024), although the QBO–MJO connection is identified to be stronger in December, January and February (Yoo and Son, 2016). Sweeney et al. (2023) also highlight a strong QBO-cloud fraction relation and suggest that the difference between QBO easterly and QBO westerly composites averaged over 10° S to 10° N results in a significant longwave cloud radiative effect (CRE) anomaly of 1 W/m2. They note that the seasonality of the QBO impact on cloud fraction is synchronized with QBO-induced variations in upper-tropospheric temperature and zonal wind.

The QBO has been proposed to modulate both dynamical and thermodynamical properties in the TTL, including temperature, static stability, and vertical wind shear, all of which influence cloud formation. Through thermal wind balance, QBO-associated variations in tropical stratospheric zonal winds drive secondary circulations that generate temperature anomalies (Plumb and Bell, 1982). The QBO westerly (easterly) phase is associated with warm (cold) anomalies in the lower altitudes. These temperature anomalies extend downwards to the upper troposphere–lower stratosphere (UTLS), altering the tropopause height, static stability, and the thermodynamic efficiency of deep convection (Collimore et al., 2003). Another suggested pathway of QBO–convection interaction is through the modulation of vertical wind shear in the UTLS.

https://doi.org/10.5194/egusphere-2026-2841
Preprint. Discussion started: 4 June 2026

Recent studies investigating high-cloud radiative feedback have employed cloud-controlling factor (CCF) analysis to better understand and constrain future projections (Wilson Kemsley et al., 2025). Here, we adopt the CCF framework to examine how the QBO modulates key meteorological controls on high clouds. Wilson Kemsley et al. (2024) have identified key controlling factors for high clouds, which are examined in this study to understand their response to the QBO, and how they modulate the QBO–cloud relationship in observations and climate models.

We apply the CCF framework in combination with ridge regression (Ceppi and Nowack, 2021) to quantify the sensitivity of high clouds to the selected controlling factors. We also examine how the QBO modulates these factors. Using both observations and CMIP6 models, this approach allows us to characterize the CCF-mediated QBO–high-cloud relationship and to diagnose the potential reasons for model bias and inter-model differences.

2 Data and Methods

The study primarily uses cloud fraction observations from Cloud-Aerosol Lidar Pathfinder Satellite Observations (CALIPSO) and climate model data from Coupled Model Inter-Comparison Project phase 6 (CMIP6). For comparison, observations from Moderate Resolution Imaging Spectroradiometer (MODIS) and International Satellite Cloud Climatology Project (ISCCP) are also briefly used. Meteorological fields, noted as CCFs, and zonal wind fields are obtained from the ERA-5 reanalysis dataset as a proxy for observations. All the datasets are used in a common temporal and spatial resolution of monthly frequency and re-gridded 5°x5° respectively.

CALIPSO was launched in April 2006 and carries the Cloud-Aerosol Lidar with Orthogonal Polarization (CALIOP) instrument that provided high-resolution (tens of metres) vertical profiles of clouds and aerosols. This active lidar sensor provides more efficient detection of optically thin clouds and multi-layer clouds compared to passive sensors. However, direct comparison of CALIPSO observations with climate model outputs is difficult because of differences in resolution, variables and so on. To address this, a reprocessed dataset called GCM-oriented CALIPSO Cloud Product (CALIPSO-GOCCP) is available (Chepfer et al., 2010).

As part of the Cloud Feedback Model Intercomparison Program (CFMIP), a CFMIP observation simulator package (COSP) (Bodas-Salcedo et al., 2011; Swales et al., 2018). has been developed to generate model diagnostics that mimic how satellites would observe the model-generated world. CALIPSO-GOCCP takes the CALIOP lidar measurements and generates outputs that is comparable to diagnostics produced by COSP. This enables a consistent comparison between observation and model-simulated clouds. The cloud detection in CALIPSO-GOCCP follows thresholds based on scattering ratio. The reprocessed data is available on a 40-level vertical grid (480m vertical spacing), comparable to the vertical resolution of GCM COSP CALIPSO data, instead of the original 30-60m vertical resolution. The specific scattering ratio thresholds and vertical averaging to produce the GCM-oriented dataset results in an underrepresentation of very thin clouds

https://doi.org/10.5194/egusphere-2026-2841
Preprint. Discussion started: 4 June 2026

in CALIPSO-GOCCP compared to standard CALIOP-NASA products. This study uses the CALIPSO-GOCCP monthly 3D cloud fraction dataset, available for 14.5 years from June 2006 to December 2020.

For comparison, observations from MODIS are also analysed. The MODIS instrument is part of the NASA mission EOS Terra and Aqua and retrieves a range of geophysical parameters including various cloud properties. The study uses monthly global gridded cloud fraction data termed MCD06COSP (Pincus et al., 2023), which combines the MODIS Terra and MODIS Aqua to produce Level-3 Atmosphere data products for COSP. 22 years of MODIS dataset are analysed from July 2002 to June 2024. Monthly cloud fraction observations from ISCCP (Schiffer and Rossow, 1983) are also shown. ISCCP data used in this study spans from July 1983 to June 2017, and we use the H-series product (Young et al., 2018). The vertical axis of MODIS and ISCCP cloud fraction datasets is cloud-top pressure (7 levels), which is the atmospheric pressure at the uppermost detected cloud top in the column, unlike vertically resolved cloud profiles from CALIPSO.

For CMIP6 evaluation, historical simulations spanning from 1850 to 2014 are used for cloud fraction and meteorological fields. 11 global circulation models (GCM) from CMIP6 have implemented the COSP ISCCP and CALIPSO simulators for cloud fraction, and 7 of those models were identified to generate a reasonable QBO. These models are analysed in this study and the mean results from these 7 models are noted as CMIP6 multi-model mean (MMM). COSP ISCCP simulated cloud fraction datasets are available at 7 cloud-top pressure levels and CALIPSO simulated cloud fraction is available at 40 vertical levels. The ISCCP high-cloud fraction suffers from biases due to unaccounted thin clouds being assigned to pressure levels above tropopause (Pincus et al., 2012), an issue that also appears in the COSP-ISCCP simulator output from model datasets (not shown). Hence for high-cloud calculations based on ISCCP simulator data, values from the lowest optical depth bin (cloud optical depth<0.3) are excluded. For the CMIP6 cloud fraction sensitivity to CCF calculations, we use 20 years of data from January 1981 to December 2000.

While we consider tropical high clouds across the region 30° S to 30° N, we will show that the QBO impact is largest in the deep tropics, and hence we report tropical-mean values for the region 10° S to 10° N. High clouds are defined as clouds with cloud-top pressure less than 440hPa as per ISCCP definition (6 km and higher for CALIPSO). As ENSO is a leading mode of variability in the tropics, to better identify the QBO impact the Niño3.4 index (Bunge and Clarke, 2009) was regressed out from all the datasets presented here.

Linear regression is employed to analyse the QBO relationship with selected atmospheric variables, and statistical significance is obtained from p-values using the Wald Test with t-distribution for the test statistic, where the null hypothesis is that the slope is zero. For MMM, significance is noted where 6 out of 7 models agree on the sign of the relationship.

https://doi.org/10.5194/egusphere-2026-2841
Preprint. Discussion started: 4 June 2026

2.1 CCF Analysis

The methodology here is motivated by the CCF analyses of Ceppi and Nowack (2021) and Wilson Kemsley et al. (2024, 2025). In the latter studies, six primary controlling factors were identified for high clouds: *surface temperature, mean upper-tropospheric static stability, relative humidity at 700 hPa (RH_{700}), vertical pressure velocity at 300hPa (ω_{300}), wind shear between 300 hPa and the surface (ΔU_{300}), and upper-tropospheric relative humidity (RH_{UT})*. RH_{UT} is defined as the vertically averaged relative humidity within the 200 hPa layer below the tropopause, calculated using the WMO definition of tropopause height (Reichler et al., 2003). As described in the Results section, while this CCF set provides reasonable results, we slightly modify it to better represent QBO-related pathways. Specifically, we replace *surface temperature* with *upper tropospheric temperature (T_{UT})*, which has been identified as a key link for the QBO–cloud relationship. We also substitute *mean upper-tropospheric static stability* with *static stability at 150 hPa (S_{150})*, consistent with recent findings highlighting this factor (Chen and Thompson, 2026). Using CCF analysis, we interpret the QBO–high cloud relationship as the product of two terms: the QBO modulation of the CCFs, versus the cloud sensitivity to meteorological factors as shown in the following equation:

$$\frac{dAMT(r)}{dQBO} = \sum_{i=1}^{M} \boldsymbol{\Theta}_i \cdot \frac{d\boldsymbol{X}_i(r)}{dQBO} \qquad [1]$$

$\boldsymbol{\Theta}_i$ represents the sensitivity of high cloud fraction ($AMT(r)$) to the i^{th} cloud-controlling factor ($\boldsymbol{X}_i$), and M is the total number of meteorological cloud-controlling factors ($M = 6$). Both $\boldsymbol{X}_i$ and $\boldsymbol{\Theta}_i$ are defined as spatial vectors over a 21 × 11 grid-box centred on r, allowing the influence of surrounding conditions to be captured instead of relying solely on local grid-point relationships. The contribution of each controlling factor to $AMT(r)$ is then obtained by the scalar product of the spatial vectors $\boldsymbol{X}_i$ and $\boldsymbol{\Theta}_i$. Slightly modifying Wilson Kemsley et al. (2025) to account for the proposed QBO-clouds mechanisms, T_{UT}, S_{150}, RH_{700}, ω_{300}, ΔU_{300}, and RH_{UT} are taken as the cloud-controlling factors $\boldsymbol{X}_i$. The $\boldsymbol{\Theta}_i$ calculation follows the ridge regression methodology introduced by Ceppi and Nowack (2021). For the models, 20 years of data from 1981 to 2000 of CCF variables and cloud fraction from the CMIP6 historical simulations are used in the $\boldsymbol{\Theta}_i$ calculation. For CALIPSO, 14.5 years of available cloud fraction data is used. ERA-5 data are used as a proxy for observations of CCF variables. To ensure that the $\boldsymbol{\Theta}_i$ calculation from CALIPSO is not biased by the shorter record length, 20 years of MODIS data are also used from comparison. The whole period of data available is used to calculate the QBO influence on CCFs employing linear regression. Convolving the terms on the RHS reconstructs the QBO–high-cloud fraction relation.

3 Results

3.1 QBO modulation of high clouds

Figure 1 illustrates the relationship between QBO and key meteorological variables in the tropical upper troposphere and stratosphere, derived from ERA-5 reanalysis data, MODIS and CALIPSO cloud observations and CMIP6 model output. The

https://doi.org/10.5194/egusphere-2026-2841
Preprint. Discussion started: 4 June 2026

QBO index is defined as the zonal-mean zonal wind at 50 hPa averaged over 10° S to 10° N. The meteorological variables are regressed onto this QBO index, with the QBO index leading by three months. Sweeney et al. (2023) showed that applying a three-month lead to the QBO index yields a significant QBO modulation of clouds extending deeper into the troposphere.

The columns display the QBO-associated anomalies in temperature, relative humidity, zonal wind, and cloud fraction, respectively. The top row shows results from reanalysis and observations (Fig. 1a–e), while the bottom row presents the CMIP6 MMM (Fig. 1f–j). Consistent with the QBO index definition, westerly zonal wind anomalies are centred at 50 hPa (first column). In both observations (Fig. 1a) and the MMM (Fig. 1e), easterly anomalies dominate the mid–upper stratosphere (above 30 hPa) whereas westerly anomalies occupy the lower stratosphere, conforming to the QBO's well-known downward propagation over time. These positive zonal wind anomalies in the lower stratosphere descend to approximately 100 hPa, although the meridional extent is slightly broader in the observations than in the MMM.

When westerly (easterly) anomalies occupy the lower stratosphere, warming (cooling) is expected in the levels immediately below, driven by the QBO-induced meridional circulation. The resulting temperature anomalies can be linked to changes in moisture, with warming typically accompanied by reduced relative humidity. These expected QBO-related temperature and humidity anomalies are evident in Fig. 1 in both observations and the MMM. During the westerly phase, positive temperature anomalies extend from ~70 hPa to below 100 hPa (Fig. 1b, g). Consistent with this warming, upper-tropospheric drying appears in the relative humidity field, with negative anomalies spanning 10° S–10° N and extending below 100 hPa, particularly in the MMM (Fig. 1c, h). However, QBO-associated temperature and relative humidity anomalies are weaker in the MMM compared to ERA-5.

Consistent with the QBO-associated warming and drying in the UTLS during the westerly phase, both observations and the MMM show a robust reduction in cloud fraction over the deep tropics (10° S–10° N). The QBO accounts for approximately 25% of the variance in tropical-mean cloud anomalies in the 14-17km layer, with the easterly phase associated with enhanced cloud fraction (Fig. S1).

The cloud fraction response to QBO in observations is analysed using MODIS and CALIPSO datasets (Fig. 1 d and e), with a corresponding CMIP6 MMM analysis using ISCCP-simulated and CALIPSO-simulated CMIP6 model cloud fractions (Fig. 1i and j). While for MODIS (Fig. 1d) and ISCCP-simulated CMIP6 data (Fig. 1i), the cloud fraction is represented as a function of cloud top pressure, CALIPSO (Fig. 1e) and CALIPSO-simulated CMIP6 (Fig. 1j) cloud fraction represents vertically resolved profiles.

https://doi.org/10.5194/egusphere-2026-2841
Preprint. Discussion started: 4 June 2026

The reduction in cloud fraction in the deep tropics extends from 100 to 200 hPa in CALIPSO (Fig. 1i). A similar vertical structure appears in both MODIS observations and the MMM (Fig. 1d, e, i, j), although the vertical extent of the significant QBO-modulated cloud fraction anomalies is not obvious in these datasets due to their limited cloud top-pressure bins. Observations also suggest a weak and largely insignificant increase in cloudiness below 200 hPa. It is evident that CALIPSO exhibits a stronger QBO–high-cloud signal than MODIS, likely because its active lidar sensor better resolves the vertical profile of thin cirrus clouds in the upper-troposphere.

For CMIP6 models, the MMM very well captures the overall reduction in tropical zonal-mean high-cloud fraction in the deep tropics above 200 hPa, despite underestimating its magnitude. However, the magnitude and vertical extent of the response vary substantially across individual models, with some simulating cloud fraction anomalies extending down to 500 hPa (Fig. S2 and S3).

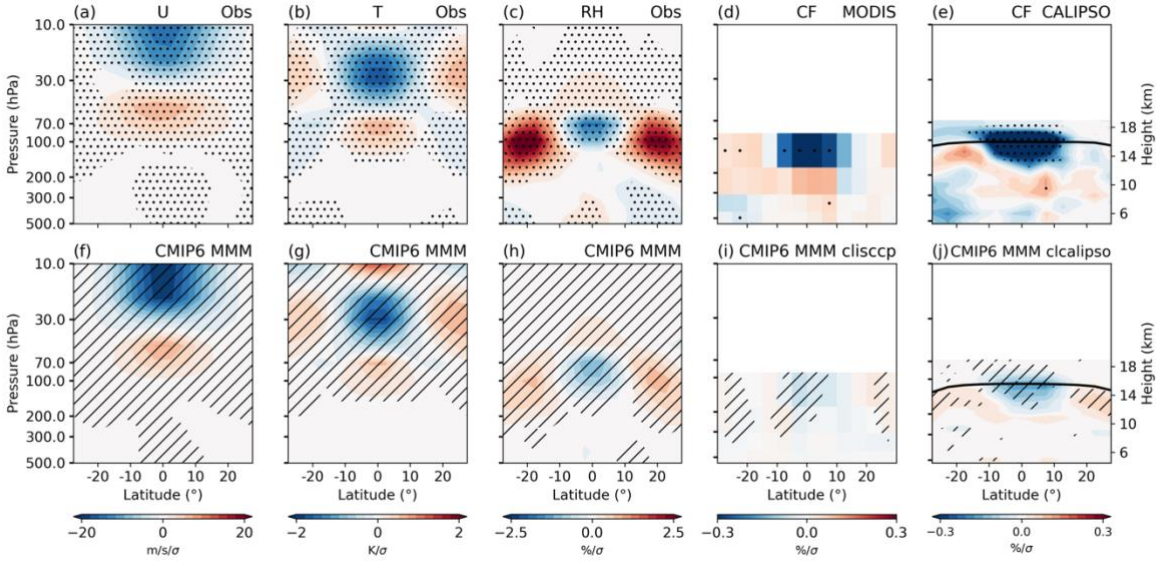

Figure 1: Latitude–height sections of QBO-regressed (a) zonal-mean zonal wind, (b) temperature, (c) relative humidity from ERA-5, (d) cloud fraction from MODIS and (i) CALIPSO between ±30 degrees latitude. (f-j) Similarly for the CMIP6 multi-model mean. Panels are shown on pressure levels, except for panels (d) and (i), which use a bin-based representation defined by cloud top pressure, and for visualisation, the uppermost bin is limited to 90 hPa. Stippling marks statistically significant results in the top row (95% confidence; 90% for cloud fraction). Hatching denotes regions where six out of seven models agree on the sign. In panels (e) and (j), the black line denotes the mean tropopause pressure level.

As both observations and models indicate a clear QBO modulation of high clouds, we now examine the latitude-longitude profile of the QBO–high-cloud fraction relation. High-cloud fraction is defined as the cloud fraction at pressure levels lower than 440hPa (above 6km), consistent with the ISCCP definition and previous studies (Wilson Kemsley et al., 2025). For

https://doi.org/10.5194/egusphere-2026-2841
Preprint. Discussion started: 4 June 2026

CALIPSO observation and MMM, which provide vertically resolved cloud fraction, Fig. 2 shows the mean cloud fraction within the selected layers. For MODIS and ISCCP (Fig. S4), which are binned by cloud-top pressure, the cloud fraction is summed across the corresponding pressure layers. Although Fig. 1 shows a clear vertical structure in the QBO–cloud relationship, we initially analyse the zonal structure of the total high-cloud fraction. This is because previous studies on the QBO–troposphere relationship have mostly focused on variables such as precipitation and outgoing longwave radiation, which may be reflected in the total high-cloud fraction (Collimore et al., 2003; Gray et al., 2018).

Although the zonal-mean high-cloud fraction shows a robust reduction during QBO westerlies, the QBO influence on high clouds and convection is not zonally symmetric (Fig. 2). Figure 2a presents the tropical distribution of QBO-regressed high-cloud fraction anomalies in observations. Consistent with Fig. 1d, the reduction in cloud fraction is most pronounced in the deep tropics from 10° S to 10° N. Across this latitude band, particularly over the oceans, cloud reductions dominate, while over the African continent, a narrow band near the Maritime Continent, and regions west of South America, localized increases in cloud fraction are evident during QBO westerlies. This spatial pattern strongly resembles results from previous regression or composite analyses of the QBO influence on outgoing longwave radiation, convective precipitation and high cloud fraction (Chen and Thompson, 2026; Collimore et al., 2003; Gray et al., 2018). Collimore et al. (2003) showed that QBO-related cloud reductions are most pronounced over regions typically occupied by deep convection. As our analysis includes thin cirrus, as well as deep convective high clouds and extended anvil clouds, background convection patterns and moisture availability likely modulate the regional QBO response. Figure S4 confirms that the zonally resolved QBO–cloud relationship is similar in ISCCP and MODIS observations as well. CMIP6 MMM roughly reproduces the observed spatial structure with a reduced high-cloud fraction during QBO westerlies in the deep tropics, but with a much weaker amplitude (Fig. 2b).

As Fig. 1 indicated the strongest cloud amount reduction above 200 hPa, instead of considering the full high-cloud fraction, we further separate the cloud fraction from 14km to 17km near the tropical tropopause layer (TTL; Fig. 2c, d) from 440hPa to 180hPa (6km to 14km) cloud fraction (Fig. 2e, f). Different from the QBO–high-cloud regression profile, a more uniform reduction in TTL clouds (14km to 17km) is evident across the deep tropics in both observations and the MMM. Overlaid contours indicate the climatology of TTL cloud fraction. In both observations and models, the climatology peaks over the Indian Ocean and the Maritime Continent, consistent with previous evidence that deep convection and TTL cloudiness peak over this region (Collimore et al., 2003; Lei et al., 2023). In observations, the strongest QBO modulation of TTL clouds also occurs over the climatology peak in the Indian Ocean, Maritime Continent and West Pacific. While the MMM reproduces the peak over the Indian Ocean (although with much weaker magnitude), the response over the Pacific is more diffuse, with a significant response towards the Central Pacific. This is because most models agree on the relationship over Indian Ocean, while Pacific responses are spread between East and West Pacific (Fig. S5). To ensure that the longer time period available for CMIP6 models does not drive the differences between models and observations, the analysis is repeated using successive

https://doi.org/10.5194/egusphere-2026-2841
Preprint. Discussion started: 4 June 2026

20-year segments of each historical model simulation. Figure S5 highlights regions where the sign of the response is not consistent across the different 20-year periods. The figure confirms that, for most models, the prominent features are robust and agree across time windows.

Recent studies have highlighted a QBO–MJO relationship, with a proposed mechanism involving the QBO modulation of clouds which could impact the radiative anomalies and hence the MJO, although uncertainties remain (Son et al., 2017; Trencham and Hood, 2024). Figure 2 indicates the QBO–cloud relationship in observations peak occur over maritime continent where the MJO activity peaks, while models fail to capture this strength in cloud modulation. This could add to the models' failure to capture the proposed QBO-MJO relationship.

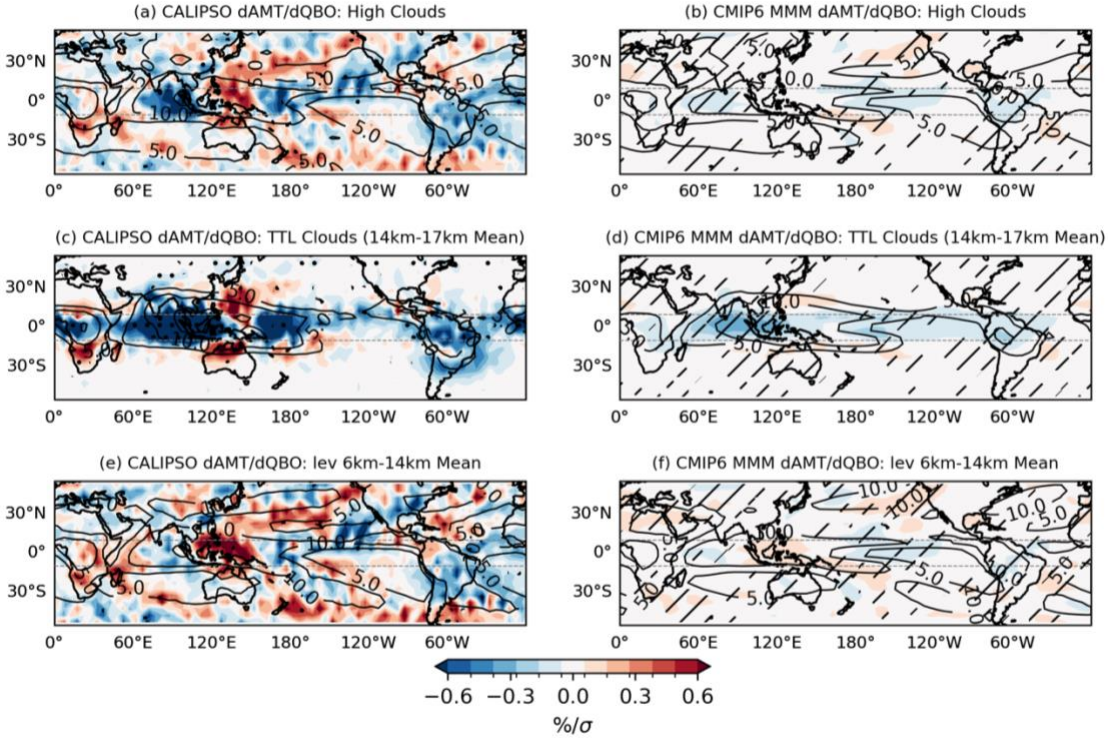

Figure 2: QBO regressed high-cloud fraction (<440hPa), TTL cloud fraction (<180hPa) and 440–180 hPa cloud fraction in MODIS (a) and CMIP6 MMM (b), represented in units of standard deviation of the QBO index. Overlaid line contours indicate the climatology of respective cloud fraction. Stippling in (a,c,e) denotes 90% confidence, and hatching in (b,d,e) denotes six out of 7 models having the same sign.

Figure 2e, f shows that, in observations, QBO westerlies result in an increase in cloud fraction in levels between 440 and 180 hPa, in most regions in the deep tropics such as over Africa, near the Maritime Continent, and the East Pacific. We note that there is little statistical significance to this relation. Unlike observations, the MMM has a much weaker response to QBO in these altitudes as well.

https://doi.org/10.5194/egusphere-2026-2841
Preprint. Discussion started: 4 June 2026

As the QBO–high cloud relationship is most prominent in the TTL, from 14km to 17km, in the following part of this study, we focus on the mechanism for the QBO–TTL cloud relationship and what causes the difference between observations and the MMM.

3.2 CCF contributions to QBO–TTL-cloud relationship

We apply the CCF framework, described in section 2, to reconstruct the spatial pattern of QBO-induced TTL-cloud anomalies shown in Fig. 2c and 2d. Figures 3a and 3b present the resulting reconstruction of QBO-regressed TTL-cloud fraction for observed and CMIP6 MMM respectively, computed using the CCF fields following equation (1). The reconstruction successfully captures the dominant spatial features of the QBO-TTL cloud relationship in both datasets. Sensitivity tests including alternative CCF combinations were also performed, such as surface temperature instead of upper troposphere temperature, and other upper tropospheric static stability indices. The current CCF set outlined in Data and Methods section provided the best agreement with the regression values.

The reconstruction captures the reduction of clouds over the Maritime Continent, stretching to the Indian Ocean and West Pacific during QBO westerlies with minor reductions over South America and the Atlantic in observations (Fig. 3a compared to Fig. 2c). The MMM reconstruction successfully captures the Indian Ocean cloud reduction and weaker reductions over the Pacific during QBO westerlies as seen in the MMM QBO-regressed TTL cloud fraction (Fig. 3b compared to Fig. 2d). Given the reasonable reconstruction using current CCFs in Fig. 3a, b, we use this framework to quantify the contribution of individual CCFs to the QBO–TTL cloud relationship.

Figure 3b-g shows the contribution of each CCF to the reconstruction of observed QBO-TTL cloud fraction relationship as shown in Fig. 3a. It is evident that the strongest drivers of the observed TTL cloud fraction reduction during QBO westerlies near the Indian Ocean and western Pacific are upper-tropospheric temperature, static stability at 150 hPa and upper-tropospheric relative humidity. While these CCFs can be correlated, since ridge regression learns separate sensitivities ($\boldsymbol{\Theta}_i$ in Eq. 1), this indicates that the clouds respond separately to local temperature (T_{UT}), static stability (S_{150}) and relative humidity (RH_{UT}). Figure S6 shows the CCF reconstruction of observed QBO-TTL cloud relationship using surface temperature ($T_{surface}$) instead of T_{UT}. The tropical-mean contribution of $T_{surface}$ to the QBO–TTL cloud relationship is almost zero, while T_{UT} drives a strong reduction in clouds (Fig. 3b; see Fig. 5b for a direct comparison with S6). And swapping $T_{surface}$ and T_{UT} had little impact on cloud sensitivities to other CCFs. This confirms that T_{UT} provides an independent contribution to the reconstruction, beyond its indirect influence through changes in static stability and relative humidity.

During QBO westerlies, warmer temperatures are present near the tropopause (Fig. 1a, f), which could increase the static stability and lead to upper tropospheric drying. Increased static stability suppresses convection, while reduced relative

https://doi.org/10.5194/egusphere-2026-2841
Preprint. Discussion started: 4 June 2026

humidity indicates decreased moisture availability for cloud formation. In addition, warming may directly influence clouds through other pathways, such as via ice cloud micro-physics or cloud-top radiative cooling. Together, all three CCFs strongly contribute to the cloud fraction response to the QBO.

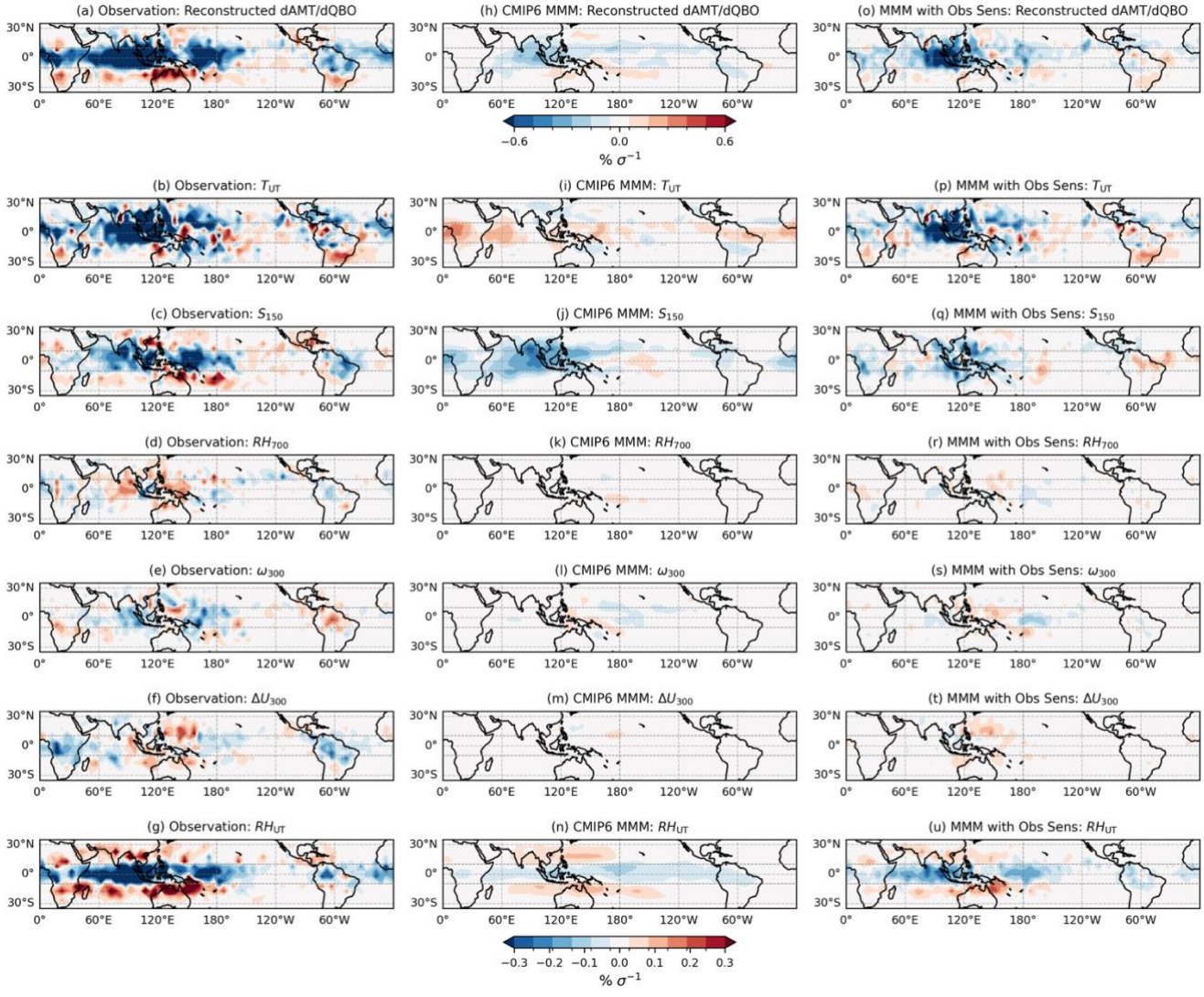

Figure 3: Reconstruction of QBO-regressed TTL cloud fraction anomalies using CCF analysis for (a) observations and (h) the CMIP6 MMM. (b-g) Contribution of each CCF to the observed QBO–TTL cloud relationship and (i-n) to the CMIP6 MMM QBO–TTL cloud relationship. (p-u) QBO-regressed CCFs from the CMIP6 MMM convolved with observed cloud sensitivities and (o) their sum.

While T_{UT}, S_{150} and RH_{UT} collectively drive the reduction in TTL cloud fraction during QBO westerlies in observations, these variables, despite being the dominant contributors, do not align spatially in the MMM (Fig. 3i-n). Although S_{150} shows a considerable contribution over the Indian Ocean in the MMM, this is not supported by corresponding T_{UT} or RH_{UT} driven

https://doi.org/10.5194/egusphere-2026-2841
Preprint. Discussion started: 4 June 2026

anomalies. Instead, the RH_{UT} mediated TTL cloud reduction peaks over the Central Pacific, while T_{UT} mostly contributes to increases in cloud fraction, and this misplaced response largely determines the spatial structure of the QBO-related TTL cloud-fraction anomalies in the MMM.

In both observations and the MMM, the remaining CCFs, RH_{700}, ω_{300} and $\triangle U_{300}$, contribute only marginally and exhibit zonally inhomogeneous signals. Although TTL clouds show strong sensitivities to these CCFs (Fig. S7c-e, i-k) – with, for example, enhanced cloud fraction with increased lower-tropospheric relative humidity or reduced cloud fraction during subsidence – the QBO induces only weak anomalies in these CCFs (Fig. S7cc-ee, ii-kk). As a result, their overall contribution to the QBO–TTL cloud relationship remains minimal. Thus, the QBO's impact on TTL clouds arises mainly from in-situ upper-tropospheric and lower-stratospheric variations rather than from surface-based processes.

To further understand why the T_{UT}, S_{150} and RH_{UT} contributions to the QBO–TTL cloud relationship agree zonally in observations, but not in the MMM, we examine the contributions of (i) the sensitivity of cloud fraction to these CCFs ($\boldsymbol{\Theta}_i$ in RHS of Eq.1) and (ii) the QBO-induced modulation of these CCFs themselves ($d\boldsymbol{X}_i(r)/dQBO$ in RHS of Eq.1). Figure 3o–u shows the reconstructed QBO-driven TTL cloud anomalies generated using observational cloud sensitivities combined with QBO-modulated CCFs from the CMIP6 models. Figure 3o reveals stronger cloud modulation near the Maritime Continent rather than over the East Pacific, with the T_{UT} (Fig. 3p) and RH_{UT} (Fig. 3u) contributions closely matching the observed spatial patterns (Fig. 3b, g). This indicates that the MMM fails to reproduce the observed zonal structure of the QBO–TTL cloud relationship primarily because of mislocated cloud sensitivities to CCFs, rather than biases in QBO signals. Note however that the QBO-modulated CCF anomalies in models are much weaker than in observations, especially for S_{150} (Fig. 3q), leading to a weaker magnitude in the reconstruction.

Figure 4a-d shows the sensitivity of cloud fraction to S_{150} and RH_{UT} in observations and the MMM, and Fig. 4e-h presents the corresponding QBO-driven CCF anomalies. Results for all CCFs, including T_{UT}, are shown in Fig. S7.

Overall, the MMM captures the expected CCF–TTL cloud fraction relationships, that is, an increase in static stability reduces cloud fraction due to suppressed convection, and an increase in relative humidity enhances cloud fraction (but not over the Indian Ocean). However, the TTL cloud fraction sensitivity to S_{150} and RH_{UT} peaks near the Maritime Continent and western Pacific in observations (Fig. 4a, c), and while models roughly reproduce this, the S_{150} sensitivities fail to peak over the western Pacific, and RH_{UT} sensitivities are weaker in the deep tropics, especially over Indian Ocean (Fig. 4b, d).

In addition, the MMM fails to capture the observed static stability response to the QBO. Observations show a pronounced increase in static stability that peaks near the Indian Ocean, the Maritime Continent and the Western Pacific during the QBO westerly phase (Fig. 4e). Models do not reproduce this pattern and show a decrease in static stability throughout the deep

https://doi.org/10.5194/egusphere-2026-2841
Preprint. Discussion started: 4 June 2026

tropics, except near the Maritime Continent (Fig. 4f). This discrepancy is likely linked to the well-known difficulty many models have in reproducing QBO signals at lower altitudes, which weakens their representation of associated UTLS stability changes. This can be confirmed from Fig. 1b and 1g, where QBO-induced temperature anomalies are weaker in the lower stratosphere in the MMM compared to ERA-5. The RH_{UT} response to the QBO is more consistent between models and observations, although observations show stronger drying in the West to Central Pacific and Atlantic (Fig. 4g), while models peak from Central to East Pacific (Fig. 4h).

Figure S6 (first raw) presents TTL cloud sensitivity to T_{UT} and the QBO-modulated T_{UT} anomalies, using a different colour scale for easier comparison. The discrepancy between observations and the MMM, as expected from Fig. 3p, primarily stems from the small sensitivity values, where the observational pattern is more spatially irregular.

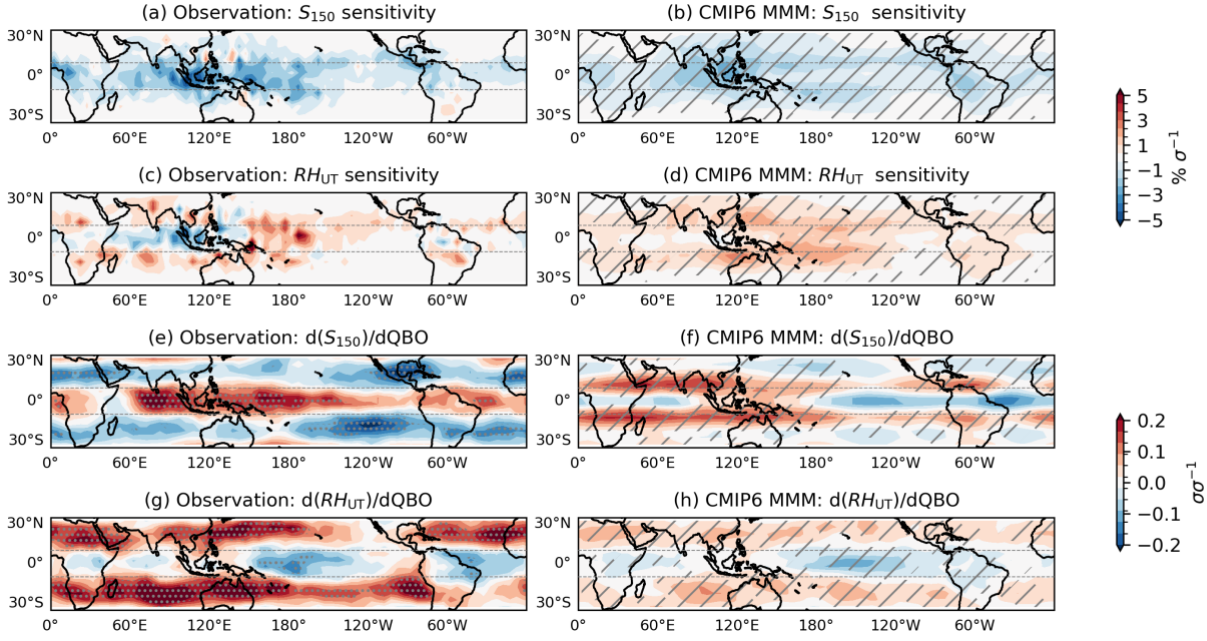

Figure 4: Historically derived sensitivities of the TTL cloud fraction to static stability at 150 hPa (S_{150}) and upper tropospheric relative humidity (RH_{UT}) in observations (a, c) and the CMIP6 MMM (b, d). QBO-regressed S_{150} and RH_{UT} respectively, in units of standard deviation of CCF per standard deviation of QBO, in observations (e, g) and the CMIP6 MMM (f, h). Stippling marks statistically significant results in the left column (99% confidence). Hatching denotes regions where six out of seven models agree on the sign.

The analysis indicates that in observations, T_{UT}, S_{150} and RH_{UT} act together to reduce the TTL cloud fraction over the Indian Ocean and western Pacific, where deep convection and TTL cloud occurrence are climatologically strongest (Fig. 2c). In contrast, the MMM shows weaker or opposite TTL cloud sensitivities to S_{150} and RH_{UT} in this region, preventing the models from reproducing the observed spatial pattern. Further, in observations, QBO-driven temperature anomalies and the

https://doi.org/10.5194/egusphere-2026-2841
Preprint. Discussion started: 4 June 2026

associated changes in static stability can effectively modulate deep convection, thereby influencing convective TTL clouds over the Maritime Continent. However, in models, the absence of robust cloud sensitivities to temperature, along with incorrect static-stability responses to the QBO limits this pathway.

3.3 Inter-model spread

While we have focused on MMM changes so far, this section explores how individual models perform in the QBO–TTL cloud relationship and the causes for inter-model spread. Figure 5a shows the tropical-mean (10° S–10° N) QBO-regressed TTL cloud fraction. Observations indicate a reduction of approximately 0.54% cloud fraction per standard deviation of the QBO index, while the CMIP6 mean reduction is around 0.12%. Although all analysed models except HadGEM3 exhibit a reduction during QBO westerlies, the magnitude of the response varies substantially across models, with CNRM-ESM2-1 exhibiting the weakest reduction and MRI-ESM2-0 the strongest reduction.

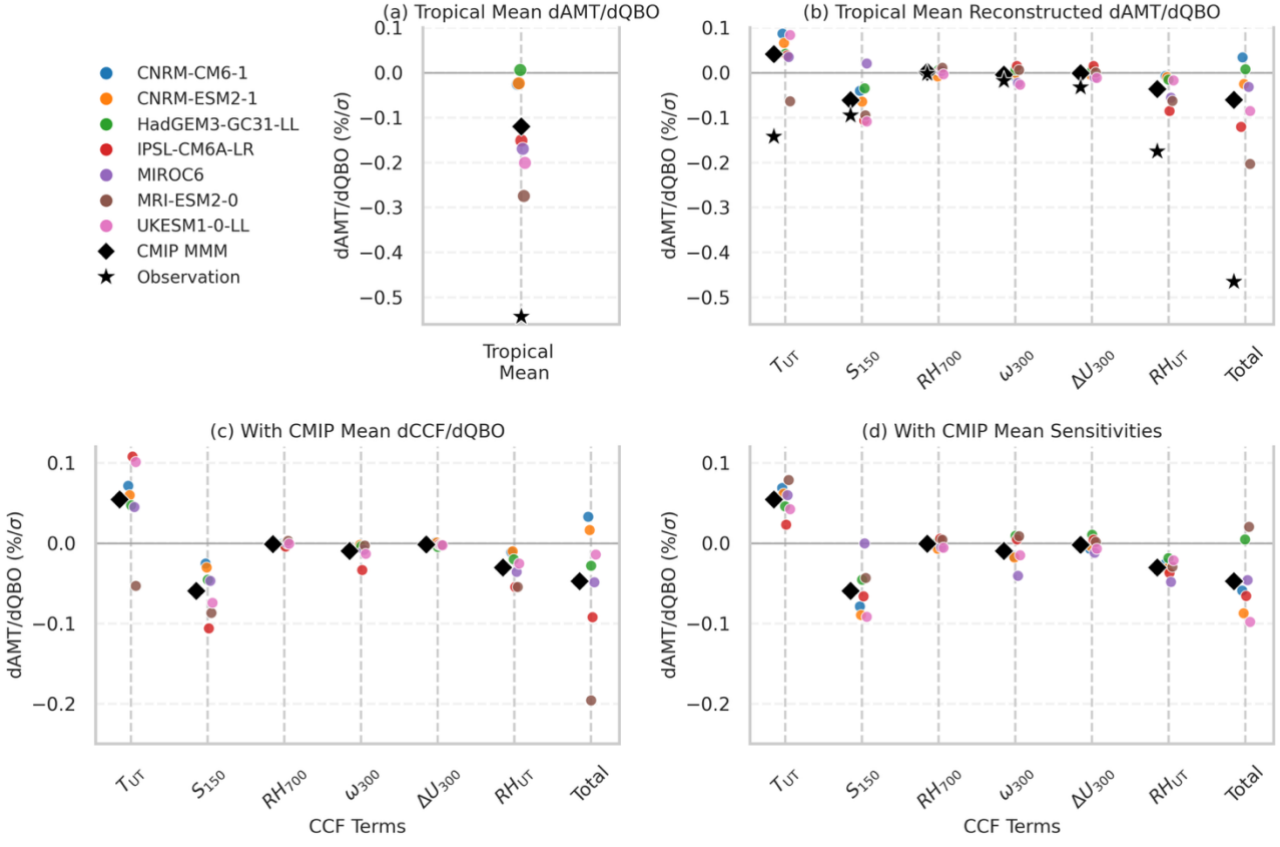

Figure 5: (a) Tropical mean (10S–10N) of QBO-regressed TTL cloud fraction in observations, CMIP6 models and the MMM. (b) Individual CCF contributions to the tropical-mean QBO-induced TTL cloud response and the total. (c) Same as (b) but replacing model-specific cloud sensitivities with the CMIP6 MMM sensitivities. (d) Same as (b) but replacing model-specific QBO-regressed CCF anomalies with the MMM CCF responses. Changes are per unit standard deviation of QBO.

https://doi.org/10.5194/egusphere-2026-2841
Preprint. Discussion started: 4 June 2026

Figure 5b presents the zonal-mean tropical-mean contribution of each CCF to the total reconstruction for observation and models. Total reconstruction and actual QBO-regressed cloud fraction in models have a correlation of 0.87 (Fig. S8). In observations, T_{UT}, RH_{UT} and S_{150} provide the dominant contributions, as noted earlier. As seen in Fig. 3, the remaining CCFs had a weaker contribution, and were zonally irregular. Hence, these dynamically localized effects largely cancel in the zonal mean and therefore contribute less to the tropical-mean QBO signal.

Consistent with observations, climate models identify T_{UT}, RH_{UT} and S_{150} as the strongest contributors towards the QBO–TTL cloud relationship. In all models, the RH_{UT} and S_{150} terms play major roles in reducing TTL cloud fraction, although the RH_{UT} contribution is much weaker compared to observations (Fig. 5b). While T_{UT} plays an important role in observations to reduce cloud fraction, TUT signals are not consistent across models, with most of them suggesting an increase in cloud fraction under this pathway.

A key question of this study is what drives the inter-model spread in the QBO–TTL-cloud relationship: differences in how models simulate the QBO modulation of CCFs, or differences in cloud sensitivities to those CCFs. To address this, we reconstruct the tropical-mean QBO-induced cloud response (as in Fig. 5b) but systematically replacing (i) model-specific cloud sensitivities with the CMIP6 MMM sensitivities (Fig. 5c), and (ii) model-specific QBO-regressed CCF anomalies with the MMM CCF responses (Fig. 5d).

Comparison of the total terms in Fig. 5c and 5d indicates that both cloud sensitivities and QBO modulation play part in the inter-model spread. In particular, the cloud sensitivities to T_{UT} and S_{150} varies substantially across models (Fig. 5c), and this variability partly explains the spread in the simulated QBO–cloud relationships. An additional contribution comes from spread in the QBO modulation of T_{UT} and S_{150}, while QBO modulation of other CCFs are broadly consistent across models (Fig. 5d). A notable outlier is MRI-ESM2-0, which exhibits a strong negative sensitivity of TTL clouds to upper-tropospheric temperature. The pronounced reduction in TTL-cloud fraction in MRI-ESM2-0 is therefore driven primarily by its strong sensitivity of clouds to T_{UT}, distinguishing it from the other models.

Overall, Fig. 5 suggests that QBO-related tropical-mean TTL cloud variability is governed mainly by QBO-induced changes in RH_{UT}, T_{UT} and S_{150}, where the latter two also constitute the dominant source of inter-model spread.

4 Conclusion

This study investigates the QBO–high cloud relationship using a CCF analysis approach applied to observations and CMIP6 climate models. While observations show that high cloud fraction in the deep tropics (10°S–10°N) is reduced during QBO westerlies, we find that CMIP6 models with a reasonable QBO also capture this relationship in the zonal mean, but

https://doi.org/10.5194/egusphere-2026-2841
Preprint. Discussion started: 4 June 2026

systematically underestimating its amplitude. Furthermore, the zonal structure of the QBO–high cloud relationship is also misrepresented, and considerable inter-model differences exist, with better agreement over the Indian Ocean and larger differences over the Pacific. The high-cloud response to the QBO also exhibits strong vertical structure, with TTL clouds (14 km to 17 km) decreasing during QBO westerlies while immediate lower-level (180–440 hPa; 6–14 km) cloud amounts show a modest increase.

We were able to reproduce the observed tropical pattern of the QBO–TTL cloud relationship using CCF analysis, with reduced cloud fraction during QBO westerlies across the deep tropics, dominated by changes over the Indian Ocean and western Pacific. We found that among the analysed CCFs, the largest contribution to the QBO–TTL cloud relationship is mediated by upper-tropospheric relative humidity, upper-tropospheric temperature and static stability at 150 hPa. Observed relationships support the theory that warmer temperatures, increases in stability and suppressed convection, and upper-tropospheric drying over deep convective regions during QBO westerlies jointly drive a reduction in cloud amount.

With a successful statistical reconstruction of the QBO–TTL cloud relationship in the models, we note that, although RH_{UT}, T_{UT}, and S_{150} remain the dominant contributors to the cloud response, consistent with observations, these contributions do not align spatially which is primarily due to mislocated cloud sensitivities. The models also underestimate the QBO-induced anomalies in these CCFs, especially in S_{150}. This could be due to the known issue of QBO signals not propagating to sufficiently low altitudes in models. Models also exhibit considerable spread in the QBO modulation of T_{UT} and S_{150}, and the TTL cloud sensitivities to T_{UT} and S_{150}, leading to substantial inter-model spread in QBO-TTL cloud relationship.

While the inability of climate models to reproduce QBO signals in the lower stratosphere is often suggested as the possible reason for biases in QBO–troposphere relationships, our study highlights that biases in TTL cloud sensitivities to meteorological factors in the models is also an equally important, if not dominant, contributor. This is consistent with the results of (Martin et al., 2021), who showed that models remained unable to capture the observed QBO–MJO relationship even with the stratosphere nudged to reanalysis fields. This suggests that other factors, such as resolution or convection and cloud parametrisations, may be responsible.

This study therefore highlights that, for models to accurately reproduce the observed QBO–TTL cloud relationship, a priority is to improve the spatial profile of TTL cloud sensitivities to the CCFs, and the QBO modulation of these CCFs needs to be stronger. While CALIPSO-GOCCP observations have limitations, and additional meteorological factors than those considered here may contribute to the QBO–cloud link, the present analysis provides a foundation for investigating how high clouds respond to a stratospheric forcing. We propose that this offers a useful framework for future analyses of the cloud response to climate change, including the contribution of greenhouse gas-driven stratospheric cooling to the cloud changes.

https://doi.org/10.5194/egusphere-2026-2841
Preprint. Discussion started: 4 June 2026

Data availability

All data used in this research is freely available. ERA5 meteorological reanalysis data are from the Copernicus Climate Change Service (Hersbach et al., 2023a, 2023b,2023c). CALIPSO-GOCCP (GCM Oriented Cloud Calipso Product) (Chepfer et al., 2010) is available at https://climserv.ipsl.polytechnique.fr/cfmip-obs/Calipso_goccp.html. Combined MODIS Aqua–Terra data are freely available and downloaded with monthly resolution (NASA, 2022). CMIP5/6 data are obtained from UK Centre for Environmental Data Analysis (CEDA).

Author contributions

AMJ and PC designed the study. AMJ conducted the analysis and produced all figures. AMJ, SWK and PC collected and processed the data. AMJ wrote the initial draft, all authors reviewed the draft and contributed to the final version of the paper.

Competing interests

PC is a member of the editorial board of Atmospheric Chemistry and Physics. Authors have no other competing interests to declare.

Acknowledgements

This work is carried out using JASMIN, the UK's collaborative data analysis environment (https://jasmin.ac.uk). Authors gratefully acknowledge World Climate Research Programme's Working Group on Coupled Modelling, which is responsible for CMIP, and the climate modelling groups for producing and making available their model output. Authors acknowledge with thanks UK Centre for Environmental Data Analysis (CEDA) and Earth System Grid Federation (ESGF) for archiving and providing access to CMIP6 model output. Authors thank the CFMIP community for providing GCM-oriented observational cloud datasets.

Financial support

AMJ was supported by Philip Leverhulme Prize funds awarded to PC. PC was supported by UK Research and Innovation (UKRI) under the UK government's Horizon Europe funding Guarantee (grant EP/Y036123/1). PC was additionally supported through UK Natural Environmental Research Council (NERC) grants NE/V012045/1 and NE/T006250/1.

https://doi.org/10.5194/egusphere-2026-2841
Preprint. Discussion started: 4 June 2026

References

Baldwin, M. P., Gray, L. J., Dunkerton, T. J., Hamilton, K., Haynes, P. H., Randel, W. J., Holton, J. R., Alexander, M. J., Hirota, I., Horinouchi, T., Jones, D. B. A., Kinnersley, J. S., Marquardt, C., Sato, K., and Takahashi, M.: The quasi-biennial oscillation, Reviews of Geophysics, 39, 179–229, https://doi.org/https://doi.org/10.1029/1999RG000073, 2001.

Bodas-Salcedo, A., Webb, M. J., Bony, S., Chepfer, H., Dufresne, J.-L., Klein, S. A., Zhang, Y., Marchand, R., Haynes, J. M., Pincus, R., and John, V. O.: COSP: Satellite simulation software for model assessment, Bull. Am. Meteorol. Soc., 92, 1023–1043, https://doi.org/10.1175/2011BAMS2856.1, 2011.

Bunge, L. and Clarke, A. J.: A Verified Estimation of the El Niño Index Niño-3.4 since 1877, J. Clim., 22, 3979–3992, https://doi.org/10.1175/2009JCLI2724.1, 2009.

Ceppi, P. and Nowack, P.: Observational evidence that cloud feedback amplifies global warming, Proceedings of the National Academy of Sciences, 118, e2026290118, https://doi.org/10.1073/pnas.2026290118, 2021.

Ceppi, P., Brient, F., Zelinka, M. D., and Hartmann, D. L.: Cloud feedback mechanisms and their representation in global climate models, WIREs Climate Change, 8, e465, https://doi.org/https://doi.org/10.1002/wcc.465, 2017.

Chen, Y.-J. and Thompson, D. W. J.: A Novel Methodology for Probing the Observed Influence of the QBO on Tropical Tropospheric Climate, Journal of Geophysical Research: Atmospheres, 131, e2025JD045491, https://doi.org/https://doi.org/10.1029/2025JD045491, 2026.

Chepfer, H., Bony, S., Winker, D., Cesana, G., Dufresne, J. L., Minnis, P., Stubenrauch, C. J., and Zeng, S.: The GCM-Oriented CALIPSO Cloud Product (CALIPSO-GOCCP), Journal of Geophysical Research: Atmospheres, 115, https://doi.org/https://doi.org/10.1029/2009JD012251, 2010.

Collimore, C. C., Martin, D. W., Hitchman, M. H., Huesmann, A., and Waliser, D. E.: On The Relationship between the QBO and Tropical Deep Convection, J. Clim., 16, 2552–2568, https://doi.org/10.1175/1520-0442(2003)016<2552:OTRBTQ>2.0.CO;2, 2003.

Davis, S. M., Liang, C. K., and Rosenlof, K. H.: Interannual variability of tropical tropopause layer clouds, Geophys. Res. Lett., 40, 2862–2866, https://doi.org/https://doi.org/10.1002/grl.50512, 2013.

Gray, L. J., Anstey, J. A., Kawatani, Y., Lu, H., Osprey, S., and Schenzinger, V.: Surface impacts of the Quasi Biennial Oscillation, Atmos. Chem. Phys., 18, 8227–8247, https://doi.org/10.5194/acp-18-8227-2018, 2018.

Holton, J. R. and Lindzen, R. S.: An Updated Theory for the Quasi-Biennial Cycle of the Tropical Stratosphere, Journal of Atmospheric Sciences, 29, 1076–1080, https://doi.org/10.1175/1520-0469(1972)029<1076:AUTFTQ>2.0.CO;2, 1972.

Kim, H., Caron, J. M., Richter, J. H., and Simpson, I. R.: The Lack of QBO-MJO Connection in CMIP6 Models, Geophys. Res. Lett., 47, e2020GL087295, https://doi.org/https://doi.org/10.1029/2020GL087295, 2020.

Lei, S., Zhu, X., Ling, Y., Teng, S., and Yao, B.: Tropical Tropopause Layer Cloud Properties from Spaceborne Active Observations, Remote Sens. (Basel)., 15, https://doi.org/10.3390/rs15051223, 2023.

https://doi.org/10.5194/egusphere-2026-2841
Preprint. Discussion started: 4 June 2026

Lim, Y. and Son, S.-W.: QBO-MJO Connection in CMIP5 Models, Journal of Geophysical Research: Atmospheres, 125, e2019JD032157, https://doi.org/https://doi.org/10.1029/2019JD032157, 2020.

Lindzen, R. S. and Holton, J. R.: A Theory of the Quasi-Biennial Oscillation, Journal of Atmospheric Sciences, 25, 1095–1107, https://doi.org/10.1175/1520-0469(1968)025<1095:ATOTQB>2.0.CO;2, 1968.

Luo, F., Xie, F., Zhou, T., Niu, Y., Xia, Y., Luo, J., Zhang, R., Wang, Y., Liang, W., and Tian, W.: The disappearing quasi-biennial oscillation under sustained global warming, Nat. Commun., 17, 2138, https://doi.org/10.1038/s41467-026-68922-2, 2026.

Martin, Z., Orbe, C., Wang, S., and Sobel, A.: The MJO–QBO Relationship in a GCM with Stratospheric Nudging, J. Clim., 34, 4603–4624, https://doi.org/10.1175/JCLI-D-20-0636.1, 2021.

Pincus, R., Platnick, S., Ackerman, S. A., Hemler, R. S., and Hofmann, R. J. P.: Reconciling Simulated and Observed Views of Clouds: MODIS, ISCCP, and the Limits of Instrument Simulators, J. Clim., 25, 4699–4720, https://doi.org/10.1175/JCLI-D-11-00267.1, 2012.

Plumb, R. A. and Bell, R. C.: A model of the quasi-biennial oscillation on an equatorial beta-plane, Quarterly Journal of the Royal Meteorological Society, 108, 335–352, https://doi.org/https://doi.org/10.1002/qj.49710845604, 1982.

Reichler, T., Dameris, M., and Sausen, R.: Determining the tropopause height from gridded data, Geophys. Res. Lett., 30, https://doi.org/https://doi.org/10.1029/2003GL018240, 2003.

Schiffer, R. A. and Rossow, W. B.: The International Satellite Cloud Climatology Project (ISCCP): The First Project of the World Climate Research Programme, Bull. Am. Meteorol. Soc., 64, 779–784, https://doi.org/10.1175/1520-0477-64.7.779, 1983.

Swales, D. J., Pincus, R., and Bodas-Salcedo, A.: The Cloud Feedback Model Intercomparison Project Observational Simulator Package: Version 2, Geosci. Model Dev., 11, 77–81, https://doi.org/10.5194/gmd-11-77-2018, 2018.

Sweeney, A. and Fu, Q.: Interannual Variability of Zonal Mean Temperature, Water Vapor, and Clouds in the Tropical Tropopause Layer, Journal of Geophysical Research: Atmospheres, 129, e2023JD039002, https://doi.org/https://doi.org/10.1029/2023JD039002, 2024.

Sweeney, A., Fu, Q., Pahlavan, H. A., and Haynes, P.: Seasonality of the QBO Impact on Equatorial Clouds, Journal of Geophysical Research: Atmospheres, 128, e2022JD037737, https://doi.org/https://doi.org/10.1029/2022JD037737, 2023.

Trencham, N. E. and Hood, L. L.: Causes of a Lack of QBO/Solar-MJO Connection in Certain CMIP6 Models, Journal of Geophysical Research: Atmospheres, 129, e2024JD041606, https://doi.org/https://doi.org/10.1029/2024JD041606, 2024.

Tseng, H.-H. and Fu, Q.: Temperature Control of the Variability of Tropical Tropopause Layer Cirrus Clouds, Journal of Geophysical Research: Atmospheres, 122, 11, 11–62, 75, https://doi.org/https://doi.org/10.1002/2017JD027093, 2017.

Wilson Kemsley, S., Ceppi, P., Andersen, H., Cermak, J., Stier, P., and Nowack, P.: A systematic evaluation of high-cloud controlling factors, Atmos. Chem. Phys., 24, 8295–8316, https://doi.org/10.5194/acp-24-8295-2024, 2024.

Wilson Kemsley, S., Nowack, P., and Ceppi, P.: Climate Models Underestimate Global Decreases in High-Cloud Amount With Warming, Geophys. Res. Lett., 52, e2024GL113316, https://doi.org/https://doi.org/10.1029/2024GL113316, 2025.

https://doi.org/10.5194/egusphere-2026-2841
Preprint. Discussion started: 4 June 2026

Yoo, C. and Son, S.-W.: Modulation of the boreal wintertime Madden-Julian oscillation by the stratospheric quasi-biennial oscillation, Geophys. Res. Lett., 43, 1392–1398, https://doi.org/https://doi.org/10.1002/2016GL067762, 2016.

Young, A. H., Knapp, K. R., Inamdar, A., Hankins, W., and Rossow, W. B.: The International Satellite Cloud Climatology Project H-Series climate data record product, Earth Syst. Sci. Data, 10, 583–593, https://doi.org/10.5194/essd-10-583-2018, 2018.